The Influence of Floodplain Restoration on Flow and Sediment Dynamics in an Urban River

Sangaralingam Ahilan
University of Leeds

Mingfu Guan
Loughborough University

Andrew Sleigh
University of Leeds

Nigel G. Wright
University of Leeds

Heejun Chang
Portland State University, changh@pdx.edu

The influence of floodplain restoration on flow and sediment dynamics in an urban river

S. Ahilan[1], M. Guan[1], A. Sleigh[1], N. Wright[2] and H. Chang[3]

1 water@leeds, School of Civil Engineering, University of Leeds, Leeds, UK
2 Faculty of Technology, De Montfort University, Leicester, UK
3 Department of Geography, Portland State University, Portland, OR, USA

Correspondence
Sangaralingam Ahilan, School of Civil
Engineering, University of Leeds, Leeds, LS2
9JT, UK
Email: s.ahilan@leeds.ac.uk;
sangar.ahilan@gmail.com

Abstract

A study of floodplain sedimentation on a recently restored floodplain is presented. This study uses a two-dimensional hydro-morphodynamic model for predicting flow and suspended-sediment dynamics in the downstream of Johnson Creek, the East Lents reach, where the bank of the river has been reconfigured to reconnect to a restored floodplain on a 0.26 km^2 (26-ha) site. The simulation scenarios include 10-, 50-, 100- and 500-year event-based deposition modelling of flood events and long-term modelling using the 64 historical flood events between 1941 and 2014. Simulation results showed that the restored floodplain significantly attenuates the upstream flood peak by up to 25% at the downstream. Results also indicated that approximately 20%–30% of sediment from the upstream is deposited on the East Lents floodplain. Furthermore, deposited sediment over the simulated period (1941–2014) is approximately 0.1% of the basin's flood storage capacity; however, the reduction in the storage does not offset the overall flood resilience impact of the flood basin. The sediment conservation at the East Lents flood basin as predicted by the model reduces the annual sediment loading of the Johnson Creek by 1% at the confluence with Willamette River, providing both improved water quality and flood resilience further downstream.

Introduction

The Pacific Northwest, like many regions of the United States has become increasingly urbanised (Yeakley *et al.* 2014) as a result of growing urban population and socio-economic development. At present more than 80% of the US population live in conurbations (U.S. Census Bureau 2010) with this value set to increase continuously. The changes in land use associated with urban development and changes in rainfall patterns are expected to increase urban flood risk (Chang and Franczky 2008) and pose a severe threat to the livelihoods and resilience of US cities. Urban flood risk is exacerbated by the fact that natural drainage systems such as floodplains are often constrained, narrowed and morphologically degraded during urban development; exposing more urban residents to floods and thus potentially make them more vulnerable to floods. Indeed, urban flood risk is function of hazard, exposure and vulnerability (Ronco *et al.* 2014). These three factors should be addressed and considered when quantifying

flood risk. Flood damage in the United States remains considerably high. Between 1985 and 2014, flooding caused an average of 82 deaths and $7.96 billion in property damage per year (National Weather Service (NWS) 2016). The Federal Emergency Management Agency (FEMA) considers flooding the number one natural hazard in the United States. In the Pacific Northwest of the United States, winter and spring flood risk in rain-snow transient basins are projected to increase in the 21st century (Dalton *et al.* 2013; Salathé *et al.* 2014).

Traditionally, urban storm water is managed with single-objective and local thinking (Christine *et al.* 2005) predominately through grey infrastructure such as embankments, sewer collection systems and, flood walls, which aim to keep floodwater away from vulnerable areas while shifting flood risk downstream (Kendrick 1988). Grey infrastructure generally fails to accommodate other aspects of integrated urban water management such as water quality, amenity, ecosystems and habitats. In addition, grey infrastructure is restricted by high capital,

maintenance and upgrade costs, and cannot be raised indefinitely in response to increasing risk (Evans *et al.* 2008). Green infrastructure such as green roofs, bio swales and floodplain restoration, enables sewer and storm water pipe drainage systems to work more effectively by reducing their operational load and the need for more expensive pipe solutions (Fletcher *et al.* 2014). It is essential to have an optimum blend of green and grey infrastructure to face current pressing urban flood risk management challenges. In recent years, making 'room for rivers' by relocating embankments, creating and increasing the depth of river channels, restoring floodplains and/or re-meandering of rivers, etc., is widely considered as a sustainable option for flood mitigation and enhanced ecosystem biodiversity (Holmes and Nielsen 1998; Rohde *et al.* 2006; Fokkens 2007).

Floodplains have profound impacts on stream flow and sediment dynamics (Holmes and Nielsen 1998; Hupp *et al.* 2009; Habersack *et al.* 2013). Floodplains serve as a form of storage during high discharge in a river and can reduce downstream flood risk (Archer 1989; Wolff and Burges 1994; O'Sullivan *et al.* 2012). Their character and evolution is essentially the product of stream power and sediment characteristics (Nanson and Croke 1992). Floodplains also provide connections between habitat areas, safe refuge for fish and wildlife, and facilitate sediment transport and storage (McIntyre and Thorne 2013). Erosion and sediment redistribution are integral, naturally-occurring components of the river system. Floodplain generally has a lower energy environment therefore sediment aggradation occurs through a combination of diffusion and convection processes over time (James 1985; Pizzuto 1987). Understanding sediment flux dynamics in an urban watershed is an important aspect for river health as nutrients, organic contaminants and heavy metals generated from industrial and densely populated urban areas can be attached to the fine sediment particles. Some of these contaminants notably pesticides, metals, and polycyclic aromatic hydrocarbons readily sorb to sediments and are able to resist degradation (Beasley and Kneale 2002).

Urbanisation affects both the volume and timing of sediment delivery in the catchment in a number of ways (Finkenbine *et al.* 2000). The excess runoff from impervious areas cause stream enlargement through bed and bank erosion and alteration of the stream bed composition (Klein 1979). Despite construction activities in the catchment generating fine sediment particles (Yorke and Herb 1978); urbanisation generally reduces the sediment delivery to the system as a result of the extent of paved surfaces in the long run. In addition, increases in paved areas shield and arrest the sources of coarse materials that have historically supplied the greater part of a system's coarse aggregate; this process results in disproportionally high levels of fine materials (silt and clays) in streams (Savage 2005). Sediment and other solid-phase constituents in rivers are considered to be the most widespread pollutant in North America by the US Environmental Protection Agency (USEPA 2000). In the United States, 13% of all rivers and 40% of impaired rivers assessed in 1998 were affected by sedimentation (USEPA 2000). Sediments can have adverse biological effects on people and habitats for fish and wildlife (Wood and Armitage 1997). High levels of sediment can cover spawning gravels, impair fish feeding and respiration, diminish food sources and decrease dissolved oxygen (DO) levels (Newcombe and Jensen 1996). Suspended solids also absorb the heat from sunlight and high concentrations may cause water temperature rise, leading to a decrease in the survival rate of fish adults and embryos (Dodds and Whiles 2004). In addition, impervious areas inhibit ground water recharge that results in low summer base flows in rivers (Klein 1979; Booth 2005), this can cause fish mortalities due to reduced velocity, cross-sectional area, and water depth (Williamson *et al.* 1993). May *et al.* (1997) reported that physical, chemical and biological characteristics of Puget Sound lowland ecoregion in the Pacific Northwest, United States continuously deteriorated with increasing urbanisation. Similarly, Singh and Chang (2014) found declining water quality in rapidly urbanising sections of small watersheds in the Portland-Vancouver, US metropolitan area.

More importantly, sediment dynamics can have considerable influence on catchment flood risk. The morphology of a river channel and its surrounding floodplain are important controls of its conveyance capacity: changes can modify the water surface elevation for a given discharge (Lane and Thorne 2007; Lane *et al.* 2007; Pender *et al.* 2016). Nevertheless, urban flood risk management has seldom taken into account the erosion, transport and deposition of sediment or the effects of flood management on sediment dynamics in the fluvial system. It is important to understand sediment dynamics in the floodplain in order to investigate its impact on flood management and vice versa. However, there are very limited studies focusing on storm-event turbidity, suspended-sediment flux dynamics and their control through green infrastructure in urban rivers, despite a number of studies elsewhere in rural catchments. This is partly because hydrological processes in urban areas need to be considered at much finer temporal and spatial scales than those in rural areas (Niemczynowicz 1999; Willems 2013). Urban hydrological applications therefore require data collection systems capable of delivering data at small spatial scale and short time resolution, which is seldom available from typical rainfall, flow and sediment monitoring stations (Roman *et al.* 2012). A considerable amount of time and expense is required for data collection and modelling work for urban catchment studies.

The aim of this study is to explore the influence of a recently restored floodplain on the flow and sediment dynamics of Johnson Creek, an urban stream known for frequent flooding and which contains sections that do not meet water quality standards under the US Clean Water Act. The study area is centred on the downstream section of Johnson Creek, the East Lents reach, where the bank of the river has been reconfigured to reconnect the river to a restored floodplain on a 0.26 km^2 site to provide more space for the river to flow and be stored. This restored floodplain can have considerable influence on sediment flux dynamics of the Johnson Creek watershed in a number of ways. Firstly, sediment trapping in the East Lents flood basin during high-flow events will reduce the overall sediment loading and catchment-wide sediment budget at the confluence with the Willamette River. Further the East Lents floodplain can have considerable impact on the erosion, transport and deposition of sediments and overall river morphology of the Johnson Creek. Secondly, we hypothesise that this sediment trapping may increase the level of contamination in the restored flood basin in long term and the potential for future remobilisation back into the river during high-flow events. However, at present, there is no field-based evidence that the sediments trapped in the East Lents floodplain pose any ecological and human health risks due to contamination. Furthermore, long-term sediment accumulation in the floodplain could result in a reduction in the design storage capacity of the flood basin.

This study investigates whether suspended-sediments from the upstream of the watershed accumulate in the restored East Lents floodplain over a period of time or flush towards to the main Willamette River. A hydro-morphodynamic model is developed to model suspended-load dominant sediment dynamics between the main channel and the floodplain, which is capable of simulating realistic patterns of overbank sedimentation on floodplains. Most of the previous sediment-related numerical modelling of floodplains are either based on a one-dimensional approach with long-term simulations (Moody and Troutman 2000; Nones et al. 2014; Pender et al. 2016) or a two-dimensional approach with the event-based simulations (e.g. Nicholas and Walling 1998; Hardy et al. 2000), they may not always realistically represent the long-term evolution of the floodplain system. In this study, both events-based and long-term two-dimensional sediment modelling is carried out to explore role of restored floodplain in short-term and long-term sediment dynamics of the river. This is the first quantitative methodology to account for long-term sediment aggradation in the restored floodplain using a two-dimensional hydro-morphodynamic model. Furthermore, floodplain influences on flood wave propagation are also explored.

Data and Methods

Study site

Johnson Creek is a 42 km (26-mile) long tributary of the Willamette River in the east of the Portland metropolitan area of the US state of Oregon (OR), serves as the study area (see Figure 1). The 140 km^2 watershed has a mixture of land uses with rural residential, forest and agriculture dominating in the upper watershed and urban areas in the middle and lower watershed. Throughout the 20th century, the watershed changed as a result of agricultural and urban development, stream channelisation, and construction of roads, storm water and sanitary systems, and other features characteristic of human occupation (Lee and Synder 2009). The river and its tributaries run through Gresham, Damascus, Portland and Milwaukie cities before discharging into the Willamette River. Johnson Creek has experienced a long history of flooding (Chang et al. 2010; Jung et al. 2011), water quality (Sonoda et al. 2001; Sonoda and Yeakley 2007; Pratt and Chang 2012; Chen and Chang 2014) and ecological problems (Hook and Yeakley 2005; Levell and Chang 2008) attributable to agricultural practices and urban development in the watershed.

Precipitation patterns in the Johnson Creek watershed are heavily influenced by Pacific storm systems that contribute to high-flow events during the late autumn and winter. Owing to the relatively small drainage area, flood peaks can occur within hours of significant rainfall, with storm runoff hydrographs generally lasting from about one to two days (Chang 2007). Over the past 80 years, there have been large-scale attempts by the City of Portland's Bureau of Environmental Services (BES) at using grey infrastructure to improve flood resilience and water quality of the Johnson Creek watershed (Savage 2005). Nevertheless, they were not as effective as expected, as flooding, water quality and other environmental issues continue to be significant problems in the watershed. These experiences reflect that working against a river's natural tendency of flow and sediment conveyance is often more costly and ineffective for a long-term solution.

In 2001, BES developed a detailed Johnson Creek Restoration Plan to improve the watershed situation for both people and the natural environment. This plan offered more emphasis on working with river natural dynamics. Subsequently, BES carried out a number of coordinated river restoration projects along the river as shown in Figure 2 that included floodplain reconnection, riparian restoration and wetland restoration.

To improve conditions for both resident and *anadromous* fish species in the East Lents reach, the bank of the river has been reconfigured to reconnect the river to a restored floodplain on a 0.26 km^2 (Figure 2). Since 1990, BES has
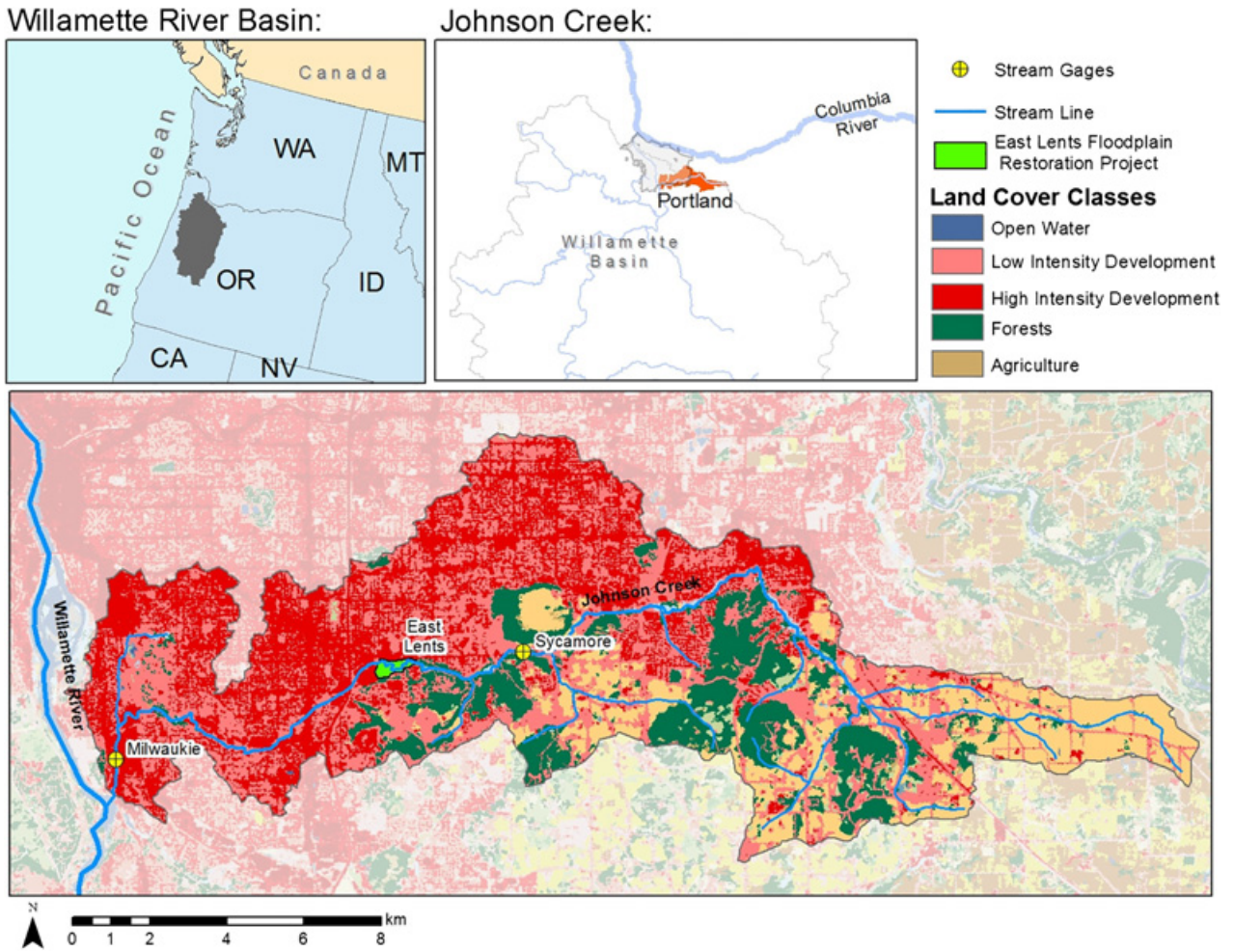
Figure 1 Johnson Creek watershed.

Figure 2 East Lents floodplain restoration.

acquired all of the property necessary for this floodplain restoration project through the Willing Seller Land Acquisition program (Yeakley and Hughes 2014). This program has helped to move people and property out of areas that frequently flood. The East Lents floodplain provides more space for the river to flow and be stored and in turn reduces the costs and damage incurred during flood events. This restoration also has helped to improve fish and wildlife habitat by increasing stream complexity, and creates passive recreational activities for city residents. The East Lents floodplain restoration was carried out in three stages: preconstruction (2010), phase I (2011) and phase II (2012).

Johnson Creek's sediment dynamics are primarily characterised by wash load transport. The major proportion of the sediment supplied to the reach is fine material (silt/clays and find sands) that mostly remains in suspension and does not interact with channel morphology. Relatively low stream power is needed to transport the fine sediment fraction; thus, sediment transport through the reach is most likely determined by the upstream sediment supply and local erosion process in the reach in the form of bank failures. The important factors primarily controlling the sediment dynamics of Johnson Creek are higher amounts of precipitation, greater slopes and a dense network of roads and ditches associated with agricultural and rural residential land uses in the upstream basin (Lee and Synder 2009). More than 70% of suspended-sediment transport in the watershed occurred during the high-flow months of November, December and January, based on the measurement of suspended-sediment concentration (SSC) between 2007 and 2010 (Stonewall and Bragg 2012). An important problem in Johnson Creek is that due to the armoring and channelization of the lower 15–17 miles of the stream, much of the sediments has a low residence time and moves quickly to the system and out to the Willamette river. Also the surrounding floodplain areas are disconnected from soil replenishment during high-flow conditions.

Flow and sediment data

The U.S. Geological Survey (USGS) have collected daily flow data from Johnson Creek since 1941 at the Sycamore (USGS #14211500) gauge that is located approximately 4 km upstream of the East Lents floodplain as shown in Figure 1. The 70 km^2 drainage area upstream of the gauge represents a majority of the contributing area for the East Lents floodplain. The U.S. Army Corps of Engineers (USACE) developed the flood frequency estimates using a log-Pearson Type III probability distribution at Sycamore gauge (USACE 1999; FEMA 2004) that are used in this study. In the first part of the study, the 10-, 50-, 100- and 500-year flood hydrographs were used in the event-based sediment simulations as shown in Figure 3.

In small rivers the annual sediment budget is mainly determined by a few extreme events related to flood and intense rainfall (Inman and Jenkins 1999). From the daily mean flow data series, 64 flood events were identified between 1941 and 2014 for long-term sediment simulation in the second part of the study. The threshold flow of 23 m^3/s (circa. 1.25-year return period) was chosen to obtain a sufficiently large number of overbank flood events that can induce floodplain sediment dynamics. The choice of the threshold (23 m^3/s) was informed by preliminary model runs. This involves systematically running a number of measured flow events (1–2 year) at the Sycamore
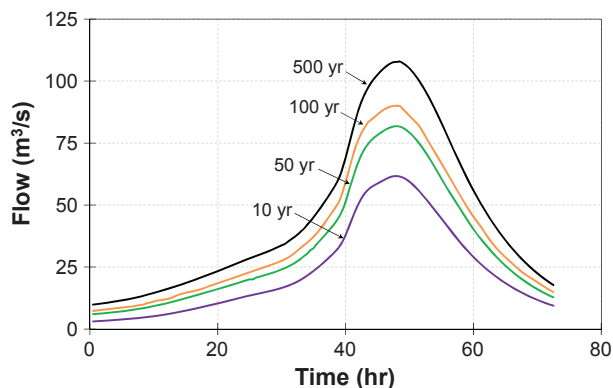

Figure 3 Flood hydrographs with different recurrence intervals.

gauging station through the hydrodynamic model to determine the threshold of the flow event which can produce overbank flow into the East Lents flood basin. The smaller events (less than 1.25-year) were excluded from a long-term simulation to reduce computational time. Data sets with greater temporal resolution (15 min/30 min/1 hr) of these 64 events were obtained from the USGS historical archives as shown in the Figure 4 for the model simulation. Prior to 1986, USGS had flow records of the Sycamore gauge in paper format; as part of this study they were systematically collated from the USGS archives. The paper records were manually scanned, interpreted and recorded into electronic format for the identified flow events. Initially, a flood water level at each time interval was estimated from each flood hydrograph from which hourly discharge was estimated based on a specific rating curve. Each rating curve was developed based on polynomial non-linear regression that best fits the measured river stage and river discharge. Since river channels change over time, separate rating curves were used for different flood events. For the earlier period prior to 1964, rating curves were derived based on the functional relationship between gauge height and discharge,
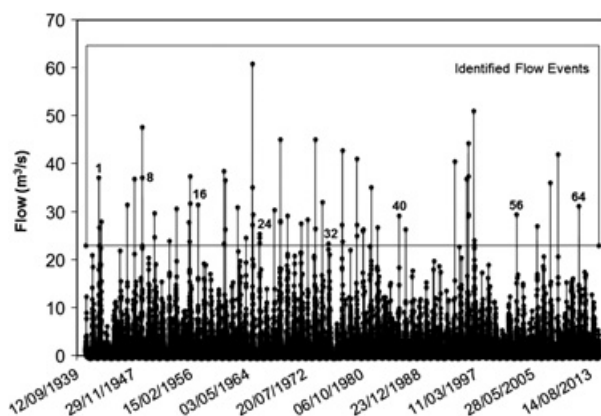

Figure 4 Time series of flow: each dot is one of the flow events identified for the long-term simulation.

while after 1964, rating curves were provided by the USGS office.

The stream slope in Johnson Creek varies considerably over its length, from 0.7% in the upper basin, to 0.34% in the mid-basin (where the study reach is located), and 1.52% in the lowest 10-km reach. The distribution of stream bottom-material particle sizes correlates with the channel slope and adjacent land use, with finer bottom-material sizes in the upper basin reach and larger material in the lower reach. The large extent of highly erodible silt-loam soil and steep slope at the upstream location produces turbidity spikes during intense rainfall events (Savage 2005).

Sediment particle size distribution plays an important role in sediment dynamics. Allen *et al.* () sampled manually a SSC at the upstream of the study region, and conducted particle size analysis using a polydisperse analysis model. The following particle sizes (D10 = 15.11 μm (fine silt), D50 = 59.98 μm (silt), D90 = 283.82 μm (fine sand)) are equally distributed as an input in the upstream boundary. In the absence of historical particle size measurements at the USGS gauging stations in the Johnson Creek watershed, we use the particle sizes above corresponding to (D90) upper bound, (D50) best estimate and (D10) lower bound to account for natural variability in particle size distribution. Stone and Droppo (1994) reported that sediment less than 63 μm in size were the dominant fraction for contaminant adsorption and transport, due to their relatively large surface area and geochemical composition. Furthermore, silt and clay are particularly important in heavy-metal transport and their storage within fluvial sediments (Thomas 1987). The flow rate is one of the primary drivers for the composition of the total SSCs in the river. At low discharge, the suspended-sediment is composed mostly of silt and clay. As discharge increases, the percentage of sand increases, while percentage of the total suspended-sediment load (SSL) consisting of silt and clay generally decreases. Based on the field measurements by the USGS in the period between 2007 and 2010, the average annual suspended-sediment yield at the Milwaukie station was 33.67 metric ton/km^2.

This study uses the USGS flow and turbidity measurements at the Milwaukie gauging station (shown in Figure 1) from December 2005 to January 2009. Generally, the total amount of sediment carried by a stream during a year is dominated by 10% or less of the days in one or several extreme events (Ashmore and Day 1988). These samples were collected primarily during large storm events, when SSCs were highest. These data sets were used to establish the relationship between stream flow and turbidity; where Q is stream flow in cubic feet per second; T is turbidity in Formazin Nephelometric Units (FNUs).

$$\log_{10} T = 0.455 \log_{10} Q + 0.947 \qquad (1)$$

In this study turbidity is used as surrogate measure for SSC. The turbidity-SSC model generally provides more reliable and reproducible SSC time series with smaller uncertainty values than other methods such as sediment transport curve using stream flow as the sole independent variable for computations of SSC or Porterfield's (1972) computational method for which there is no quantitative method for deriving uncertainty (Rasmussen *et al.* 2009). This approximation can also have some inherent limitations as turbidity not only depends on the SSCs but also depends on particle size distribution and shape of suspended-sediment particles (Bilotta and Brazier 2008). However, in this case, since nearly all particles are sand and silt moving in suspension, this assumption is deemed to be adequate.

As part of the USGS investigation on suspended-sediment characteristics of the Johnson Creek basin, Stonewall and Bragg (2012) established the following relationship amongst *SSC*, in mg/l, *T*, and *Q* based on the 2007–2010 data sets at the Milwaukie gauging station.

$$\log_{10} \text{SSC} = 1.024 \log_{10} T + 0.143 \log_{10} Q - 0.419 \qquad (2)$$

In the absence of sediment data in the nearby upstream location, an input to the model was developed based on the relationship of stream flow and turbidity to suspended-sediment at the Milwaukie station which is located in the downstream of the study reach. A computed SSC time series which was derived based on Eqns (1) and (2) was translated into the SSL by dividing the SSC by the density of the sediment. The paired stream flow and SSL data sets were used as an input to the model.

Topography data sets

The Digital Elevation Model (DEM) data sets with a resolution of 1.5 m × 1.5 m obtained from the BES (Bureau of Environmental Services, City of Portland) were used to define the topography of the study region. In addition, a surveyed data set at approximately 30-m intervals along the river was obtained from existing HEC-RAS model of the East Lents reach (Timmins and Wolff 2012) and used to adjust the river channel and bank elevations. Interpolation of these data enabled the construction of a discretised grid with a nodal spacing of 1.5 m. This scale of resolution allowed complex topographic features to be represented by the grid with minimal loss of detail. In both event-based and long-term simulations, the existing DEM was used to represent the starting point.

Model setup

A layer-based hydro-morphodynamic model developed by Guan et al. (2014, 2015a, 2015b) was used to model

suspended-sediment dynamics between the main channel and the floodplain. The model encompasses three modules: a hydrodynamic module governed by the two-dimensional shallow water equations, a sediment transport module, and a morphological evolution module for updating the bed elevation due to erosion and deposition. Because sediment transport in the Johnson Creek is predominately characterised by wash load transport, a suspended-sediment module was considered in this study. This study primarily focused on the amount of suspended-sediment trapped in the floodplain rather than the internal bed modifications in the East Lents flood basin. During phase I and phase II of the restoration; 90,000 seedlings of the native trees and shrubs were planted in the East Lents flood basin. As shown in Figure 2, the East Lents flood basin is densely covered by vegetation therefore it is assumed that the original floodplain is immobile in this study. Furthermore, as part of the East Lents floodplain restoration, the banks of the East Lents reach have been protected and confined. The amount of the stream that is freely able to deform banks of its reach is quite limited. Therefore, this study did not account for morphological changes of the river channel in the event-based or long-term simulations.

Hydrodynamic model

The hydrodynamic model is based on two-dimensional shallow water equations with the exchange of sediment transport and water. Following Guan *et al.* (2014, 2015b), the governing equations can be expressed in details by:

$$\frac{\partial \eta}{\partial t} + \frac{\partial hu}{\partial x} + \frac{\partial hv}{\partial y} = 0 \tag{3}$$

$$\frac{\partial hu}{\partial t} + \frac{\partial}{\partial x}\left(hu^2 + \frac{1}{2}gh^2\right) + \frac{\partial huv}{\partial y} = gh\left(S_{ox} - S_{fx}\right)$$
$$+ h\nu_t\left(\frac{\partial^2 u}{\partial x^2} + \frac{\partial^2 u}{\partial y^2}\right) + \frac{(\rho_0 - \rho)u}{\rho}\frac{\partial z_b}{\partial t} - \frac{\Delta\rho gh^2}{2\rho}\frac{\partial C}{\partial x} \tag{4}$$

$$\frac{\partial hv}{\partial t} + \frac{\partial huv}{\partial x} + \frac{\partial}{\partial y}\left(hv^2 + \frac{1}{2}gh^2\right) = gh\left(S_{oy} - S_{fy}\right)$$
$$+ h\nu_t\left(\frac{\partial^2 v}{\partial x^2} + \frac{\partial^2 v}{\partial y^2}\right) + \frac{(\rho_0 - \rho)v}{\rho}\frac{\partial z_b}{\partial t} - \frac{\Delta\rho gh^2}{2\rho}\frac{\partial C}{\partial y} \tag{5}$$

where t, time, in second; g, gravitational acceleration in m/s^2; η, water surface in m; z_b, bed level in m; $h = \eta - z_b =$ flow depth in m; u, v, depth-averaged flow velocities in x and y direction in m/s; ν_t = turbulent viscosity coefficient;

C = total volumetric sediment concentration $C = \sum_{i=1}^{N} C_i$,

where C_i = volumetric concentration of the ith class by suspended load; $\Delta\rho = \rho_s - \rho_w$, ρ_s, ρ_w, density of sediment and

water flow respectively (m^3/s); ρ, bulk density of sediment and flow mixture in m^3/s $S_{ox} = -\partial z_b/\partial x$, $S_{oy} = -\partial z_b/\partial y$, bed slopes in the x and y direction respectively; S_{fx}, S_{fy} are frictional slopes in the x and y components which are calculated based on Manning's roughness coefficient n.

Suspended sediment load model

The suspended load transport is governed by the advection–diffusion equation. For non-uniform graded sediment mixtures, it is necessary to divide the graded sediments into fractions due to the difference of grain-size related parameters. Following Guan *et al.* (2015b), for the suspended transport of each fraction, the governing equation is described by

$$\frac{\partial hC_i}{\partial t} + \frac{\partial huC_i}{\partial x} + \frac{\partial hvC_i}{\partial y} = \frac{\partial}{\partial x}\left(\varepsilon_x h \frac{\partial C_i}{\partial x}\right) + \frac{\partial}{\partial y}\left(\varepsilon_y h \frac{\partial C_i}{\partial y}\right)$$
$$+ (S_{E,i} - S_{D,i}) \tag{6}$$

where ε_x, ε_y, diffusion coefficients of sediment in the x and y directions, respectively; $S_{E,i}$, entrainment flux of sediment for the ith fraction; $S_{D,i}$ deposition flux of sediment of the ith fraction. As there is no universal theoretical expression for the vital entrainment flux and deposition flux of sediments, both variables are calculated by the following widely-used function.

$$S_{E,i} = F_i \omega_{f,i} C_{ae,i}; \; S_{D,i} = F_i \omega_{f,i} C_{a,i} \tag{7}$$

where F_i, percentage of the ith grain fraction; $\omega_{f,i}$, effective settling velocity for the ith grain fraction which is calculated by using the formula derived by Soulsby (1997):

$$\omega_{f,i} = \frac{\nu}{d_i}\left[\sqrt{10.36^2 + (1-C)^{4.7}1.049 d_{*,i}^3} - 10.36\right] \tag{8}$$

where $d_{*,i} = d_i\left[\frac{g(s-1)}{\nu^2}\right]^{1/3}$; $C_{a,i} = \delta C_i$ is the near-bed concentration for the ith grain fraction at the reference level a; the definition of the coefficient δ is: $\delta = \min\{2.0, (1. \text{ p})/C\}$; $C_{ae,i}$ is the near-bed equilibrium concentration at the reference level that is calculated by using the van Rijin's formula (van Rijin 1984; Guan *et al.* 2015a).

Morphological evolution model

Morphological evolution is determined by the difference of sediment entrainment and deposition that is calculated per grid cell at each time step. The equation used to calculate morphological change is written by:

$$\frac{\partial z_b}{\partial t} = \sum_{i=1}^{N} \left(\frac{\partial z_b}{\partial t}\right)_i = \frac{1}{1-p} \sum_{i=1}^{N} (S_{D,i} - S_{E,i}) \qquad (9)$$

where p is porosity and N is the number of grain-size fractions, here $N = 3$.

Morphodynamic simulations of multi-year events were carried out for the identified 64 flood events, (Figure 4). Since these flood events occurred in different time periods, the hydro-morphodynamic model was modified to account for this time lag. At the end of each simulation, a sufficient time of around 2 hr was allowed for almost all of the suspended-sediments in the water column to settle down in the basin. The water level was then set to zero to ensure that the floodplain was dry prior to the next flood event simulation. This long-term simulation allowed a detailed investigation of the sediment dynamics in the flood basin with the sequence of historical flooding.

Results and Discussions

Hydrodynamic model simulations

Off-channel storage of flood waters in the East Lents flood basin has a significant attenuation effect on upstream hydrographs (Figure 5). Simulation results show that the volume difference between the inflow and outflow hydrographs for 10- and 500-year flood events are (4.4×10^5) m³ and (1.9×10^6) m³, respectively, which includes flood basin storage of (1.37×10^5) m³ and (1.69×10^5) m³. The remaining flood volume of (3.03×10^5) m³ and (1.73×10^6) m³ gets into the Foster road through north open boundary of the model (Figure 2 and Figure 7). At the end of the flood event, the outflow matches the inflow because the storage that occurs during the flooding is retained in the East Lents floodplain (Figure 5). This is because the East Lents flood basin acts as a form of storage reservoir. There is a floodgate in place on west side of the floodplain to release part of the flood storage back to the Johnson creek in a control manner further upstream of the study region, but this release is not included in the model as it is not pertinent to the study. The difference in the peak flow of the upstream and downstream hydrographs is expressed in terms of % relative attenuation:

$$\% \text{ Relative attenuation} = \frac{Q_{P1} - Q_{P2}}{Q_{P1}} \times 100 \qquad (10)$$

where Q_{P1} and Q_{P2} are the peaks of the inflow and outflow hydrographs in Figure 5. This off-line storage provides
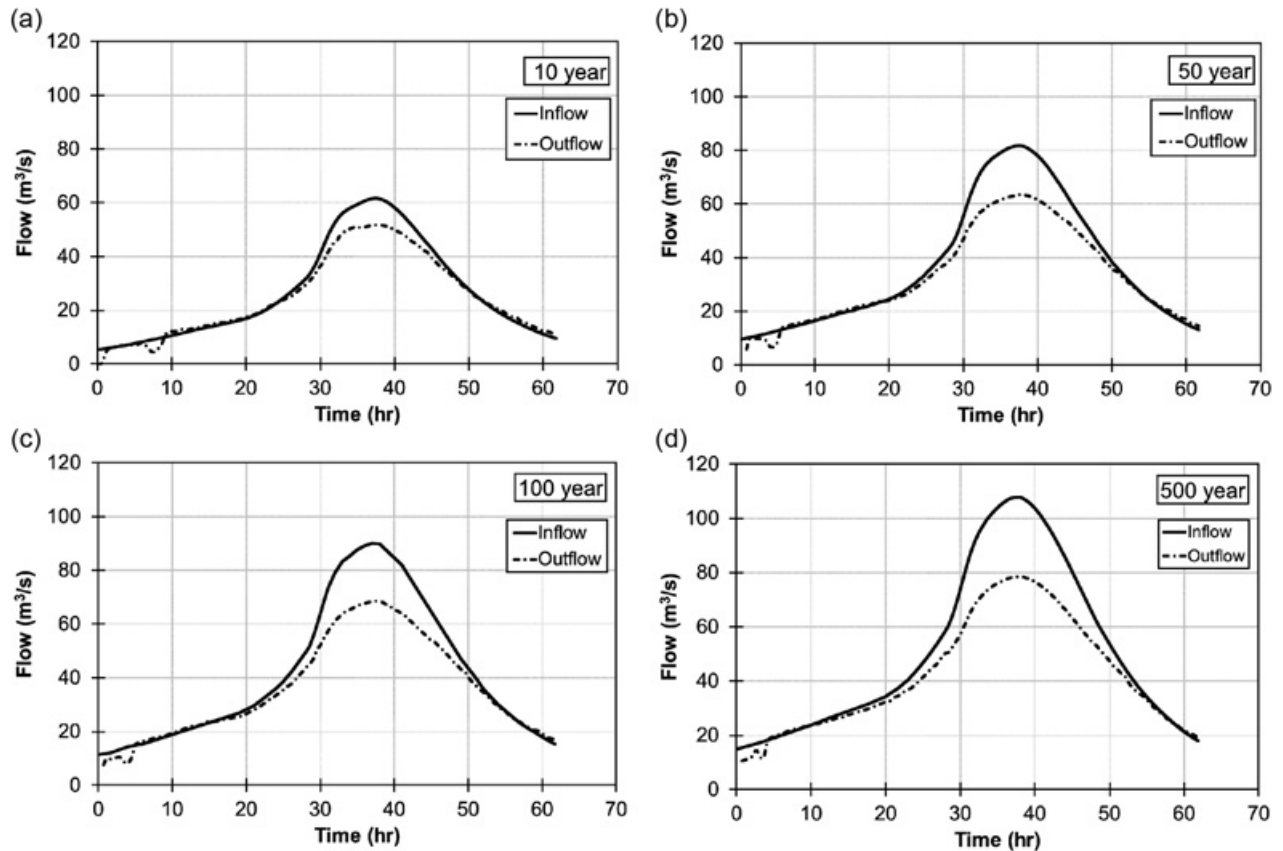

Figure 5 Inflow and attenuated outflow hydrographs of the (a) 10-year, (b) 50-year, (c) 100-year and (d) 500-year flood events.

reduction in flood peak of 16% and 27% for 10- and 500-year flood events, respectively. Furthermore, the peak flow of 500-year flood hydrograph was reduced to approximately 80 m³/s, which is equivalent to peak flow of 50-year flood. This implies the significant benefit of the floodplain storage on flood peak attenuation.

At the beginning relative attenuation decreases with discharge up to 2-year flow events (Figure 6), this could be partly due to scatter. Other possible explanation for this trend includes, in the beginning a significant proportion of the smallest flow is contributed to fill up the available depression storage in the floodplain. When flow increases, these impacts on overbank flow are diminished as most of the depression storage is filled with relatively smaller proportion of flow. However, during the higher overbank flow (>2-year) events, the flood basin is active in providing significant flood storage and attenuates the propagation of flood wave along the channel. The largest historical event occurred on December 22, 1964 and experienced 23% reduction in the flood peak magnitude at the downstream.

This result differs from previous research findings. Woltemade and Potter (1994) reported that in the Grant River watershed, southwestern Wisconsin, USA, the attenuation of moderate volume flood events (5–50 year) with relatively high peak-to-volume ratios, was significantly influenced by floodplain storage. They also stated that as flows continue to increase to values in return periods greater than 50-year, flood attenuation was shown to decrease and then approach to a nearly constant value. They suggested that, during higher flow events, most of the floodplain elements such as emergent or surface penetrating vegetation were overtopped, and the available depression storage was filled up. Consequently, the flood waves propagated rapidly down the valley with lower attenuation in the flood peak. O'Sullivan et al. (2012) carried out a detailed empirical study to determine the impact of floodplain and hydrograph properties on flood wave propagation. Their simulation results
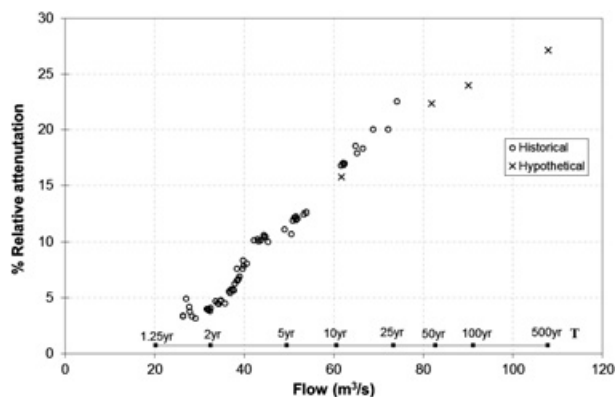
indicated that (2-25 year) flood events experienced relatively significant delays and the flood peak attenuation occurred at the downstream of the floodplain.

The primary reason for this counter-intuitive behaviour is due to alignment and geomorphic setting of the East Lents floodplain (Figure 7). The site's landscape is rather unique given that the pre-historic and catastrophic Missoula Flood events of about 10,000 years ago played a major role in its formation. Much of the floodplain in this area is actually lower than the top of bank which creates substantial off-line storage, the East Lents restoration enhance that the stream is able to access this natural storage.

The floodplain behaves in some way more like an alluvial fan than floodplain in the typical sense, therefore, it is still active and can provide 28% flood peak attenuation for 500-year flood event. The common assumption that hydrologic restorations are only effective for small or medium flow events (Wolff and Burges 1994; Woltemade and Potter 1994; O'Sullivan et al. 2012) does not always hold, because, this primarily depends on the system's geomorphic configurations and hydrograph characteristics. Despite the fact that the hydrodynamic model simulates floodplain inundation of the East Lents flood basin reasonably well, there are a few inherent limitations in this study (e.g. the bed terrain resolution, boundary setting). In this study, a 1.5 m resolution DEM was used to capture the flow and sediment dynamics; this resolution may however miss the flood and sediment storage in smaller localised depressions in the flood basin. In the study, details of the pipe networks were not incorporated in the flow boundary settings.

Morphodynamic model simulations

The spatial variation of simulated sediment deposition of different flood events is shown in the Figure 8. As expected, scale of sediment deposition in the floodplain increases with flood magnitude. The larger events bring higher overbank flow and sediments into the flood basin. Figure 8 also
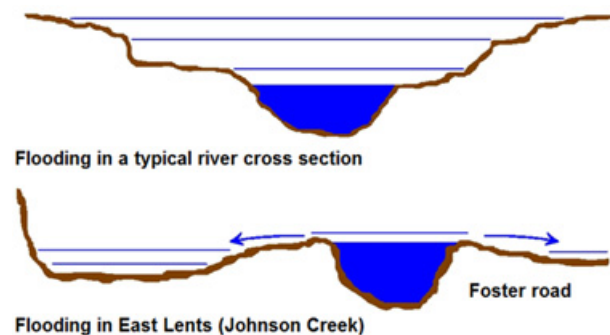

Figure 6 Relative attenuation of the 64 historical and four hypothetical flood (10-, 50-, 100-, and 500-year flood) events.

Figure 7 Flooding in a typical river cross section and in East Lents.
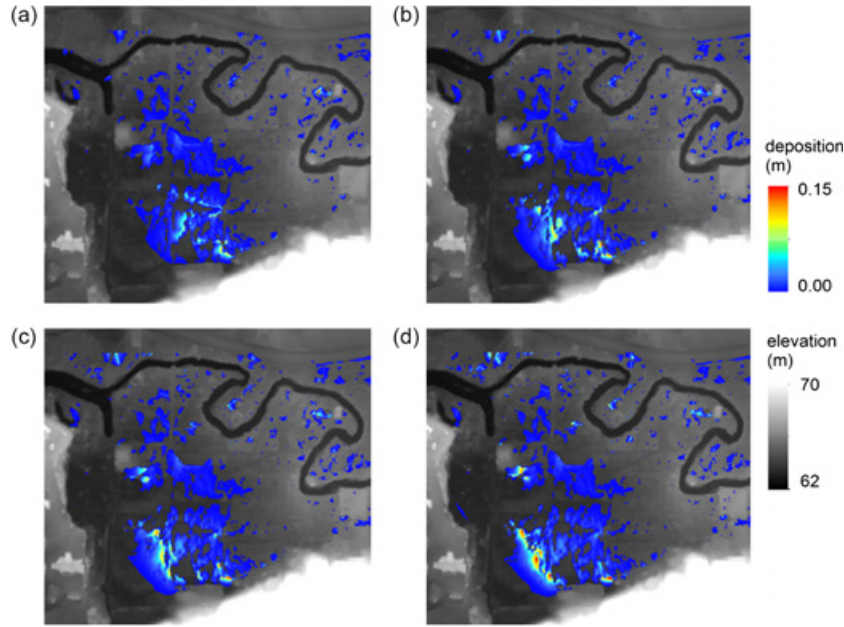
Figure 8 Sediment depositions for (a) 10-year, (b) 50-year, (c) 100-year and (d) 500-year flood event.

shows sediment deposition moves towards the lower elevation of the floodplain in the southwestern direction with flood magnitude as it has low energy environment. The higher ground along the western boundary of the mapped area is mostly artificial fill. In predevelopment times, flood flows used to flow overland to the southwest but are now constrained by the land fill and so are forced to pond. Table 1 compares cumulative amount of sediment deposited into the basin with the total SSL input upstream.

As shown in the Table 1, circa. 30% suspended-sediment that comes from the upstream was deposited in the East Lents flood basin over the four simulated flood events. The amount of sediment deposited in the floodplain is mainly driven by the volume of overbank flow that gets on to the floodplain and as the floodplain aggrades, the inundation frequency and duration changes. The amount of sediment deposition increases with flood magnitude but the percentage of the sediment trapped in the floodplain almost remains constant when compared with total suspended-sediment input. Figure 9(a) and (b) shows the temporal variation of input SSC at the upstream and the cumulative deposition volume in the floodplain during the flooding

respectively. As SSC is derived from the discharge (Q) through regression relationships, Figure 9(a) offsets the discharge curve (Figure 3).
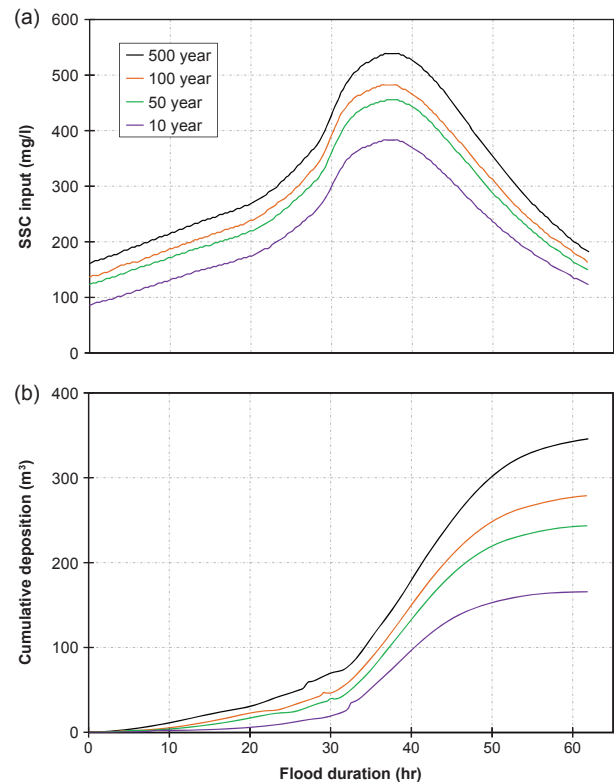

Figure 9 (a) Suspended-sediment concentration (SSC) input and (b) Cumulative Sediment deposition.

Table 1 Sediment mass balance for different flood events

	10-year	50-year	100-year	500-year
Input (SSL m^3)	630.74	1040.32	1241.35	1687.62
Deposited in the floodplain (SSL m^3)	203.24	300.67	379.62	490.51
% SSL deposit	29.06	30.58	28.90	32.22

SSL, suspended-sediment load.

As shown in the Figure 9(a), the SSC increases with magnitude of the flood event, the average SSC for (10–500 year) return period events vary from 227 mg/l to 337 mg/l. The severity of effect of suspended-sediment on fisheries is a function of SSC and exposure time. These concentrations with exposure time 60 hr make a severity-of-ill-effect score between 7 and 8 along a 15-point scale (Newcombe and Jensen (1996) for juvenile salmonids (Chinook salmon, Rainbow trout and Mountain whitefish). Although this level of score is not high enough for fish mortality, this can cause increased physiological stress on juvenile salmonids and make them to migrate to other location. Figure 9 (b) shows cumulative sediment deposition in the floodplain with flood duration. The cumulative sediment deposition follows the SSC input and higher rate of deposition occurred on the recession limb of the hydrograph as this phase provides low energy environment for sediment to settle. The similar morphodynamic simulations were carried out for flood events between 1941 and 2014. The temporal and spatial changes of the floodplain topography as a result of cumulative sediment deposition at regular intervals are shown in Figure 10.

As expected, the amount of sediment accumulated in the flood basin gradually increases with subsequent flooding. While the largest flood event in the study period occurred on December 22, 1964, there is little noticeable change in sediment deposition depth between Figure 10(c) and (d). This is because deposited sediments are partially re-suspended during the large flood events (>25-year) and re-deposited in different locations in the floodplain rather than accumulating in specific locations. However, the medium range flood events (5- to 25-year return period)
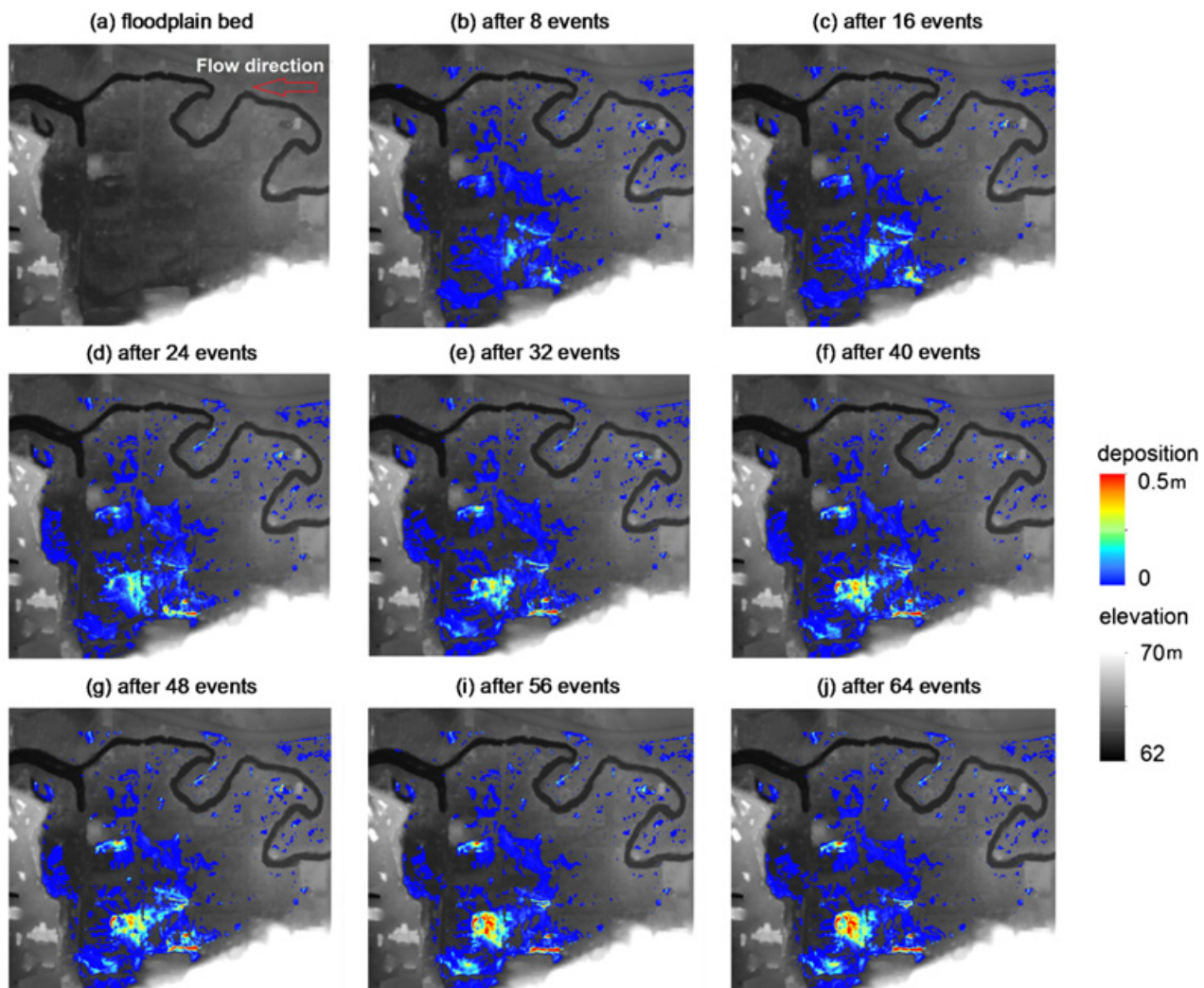

Figure 10 Cumulative sediment depositions after 8, 16, 24, 32, 40, 48, 56 and 64 events.

are primarily causing sediment hotspots in the flood basin since, during medium flood events, sediments tend to concentrate at specific locations rather than being redistributed across the basin. The smaller events (less than 5-year return period) have little effect on the overall sediment dynamics of the basin as they produce relatively small overbank flow and sediment contributions to the floodplain. As shown in Figure 9, the area of deposition shifts towards the lower elevation of the basin in the south west direction.

The deposition and re-suspension process is also represented in Figure 11 that illustrates the temporal cumulative sediment deposition in the floodplain over the long-term simulation of 64 historical flood events. The large flood events bring a greater amount of sediments into the basin as there is adequate overbank flow to transport the sediment. Figure 11(a) shows that after each flood there is a drop in accumulation of sediment volume because the next flood re-suspended the accumulated sediments.

At the end of the long-term simulation, 2,000 m^3 of sediment has been deposited in the flood basin which is equivalent to 0.4 metric ton/km^2 at the Sycamore gauging station. In other words, the sediment trapping at the East Lents flood basin reduces the annual sediment loading of the Johnson Creek by 1% into the Willamette River, this provides both water quality and flood resilience benefits. Furthermore, deposited sediment over the simulated period (1941–2014) is approximately 0.1% of the basin's storage capacity. In order to investigate the impact of loss in floodplain storage capacity, four hypothetical (10-, 50-, 100- and 500-year) flood events are routed through East Lents reach with deformed floodplain and compare with the pre-sedimentation flood simulation results (Figure 12).

As shown in the Figure 12, flood peaks are slightly increased as a result of the long-term sediment deposition for all flood events up to 1.5%. However, its effect on existing downstream flood resilience is marginal. This is due to deposited sediment volume being relatively insignificant when compared with the flood basin storage capacity.

Our simulated results are well supported by empirical evidence. In December 2015, heavy winter storms brought floods in several places of the Pacific Northwest of United States. Johnson Creek at Sycamore gage had a new flood stage record, surpassing the 1996 flood. While Johnson Creek did flood during this storm event, the restored East Lents floodplain evidently provided enough space for water, a space to fill the 0.26 km^2 (63-acre) area with 60 cm of water. As a result, the Foster road next to the restoration site did not flood to nearly the same extent as in previous years, reducing the extent of flood. However, the further downstream sections of Johnson Creek was still briefly flooded, demonstrating the need for further restoration of wetlands and floodplain along the creek.
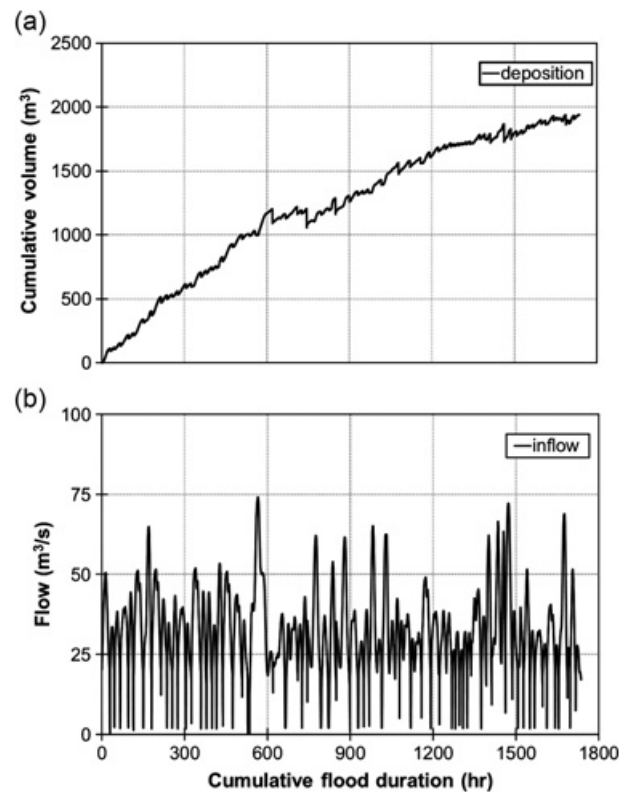

Figure 11 (a) Cumulative volume of sediment deposition in the floodplain and (b) inflow.

The morphological modelling approach inevitably has a few inherent limitations. Although data sets were collated as part of the study, there are some limitations in the available data. These included the absence of suspended-sediment measurements at the upstream of the study location and the use of a single sample to determine the particle size distribution of the suspended-sediment. Further, non-availability of survey data sets since the East Lents flood basin restoration was not enable to verify the morphodynamic simulation results. The primary focus of this study is on the suspended-sediment dynamics of the East Lents floodplain. Bed load sediment dynamics channel and the floodplain were not considered in the study. In the long-term sediment modelling, due to computational limitations, the timeframe between events and the colonisation–immobilisation potential of new deposits were not taken into account. Further to model morphological change, empirical parameters such as entrainment and deposition flux are necessary. For example, the changes of bed elevation were directly determined based on the entrainment and deposition flux of suspended load; however, all existing functions were empirically produced based on the experimental data, and these limitations could result in uncertainty in terms of the simulated bed changes.
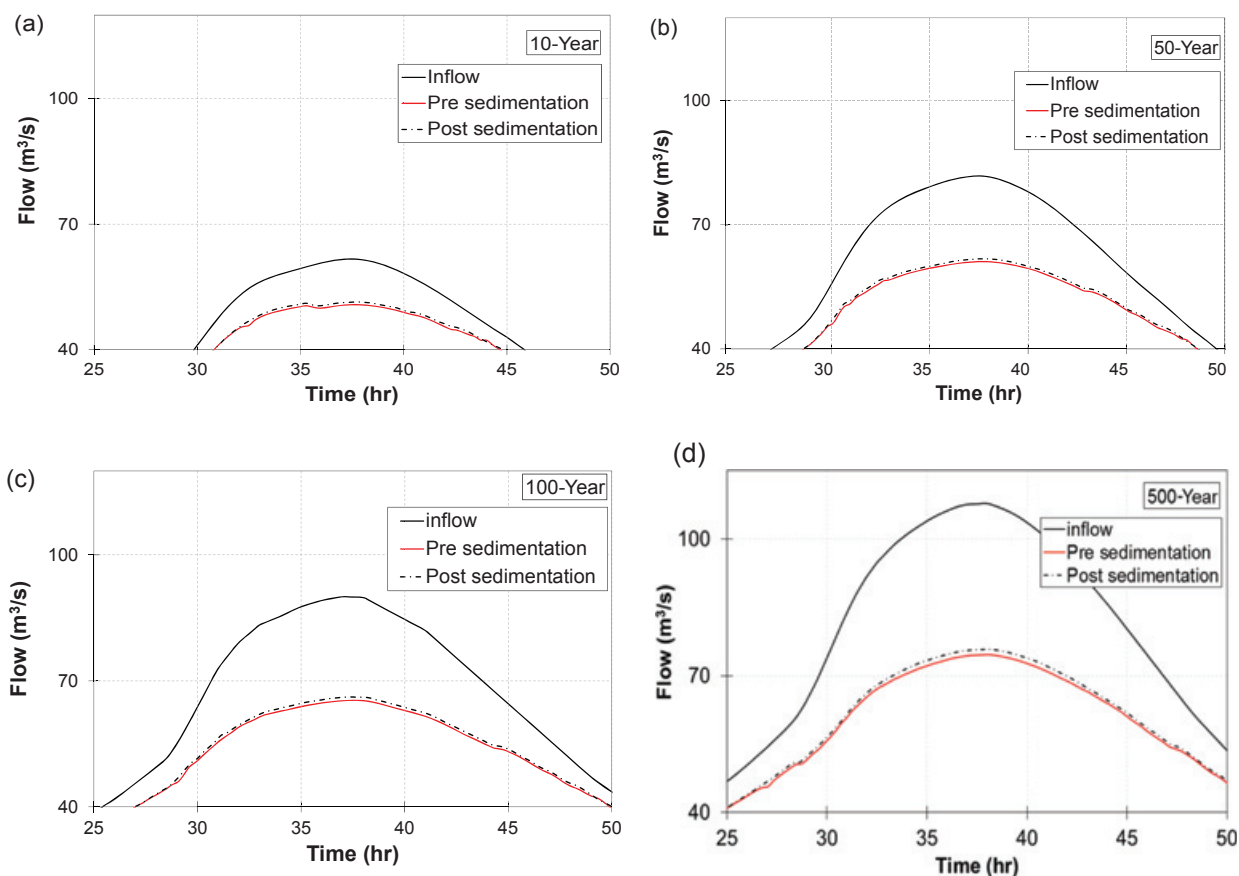
Figure 12 Inflow and attenuated hydrograph 'with' and 'without' floodplain sedimentation.

Conclusions

The application of a two-dimensional hydro-morphodynamic model to the Johnson Creek, the East Lents reach demonstrates that floodplain restorations can have a pronounced effect on flood and sediment dynamics. The simulation scenarios include 10-, 50-, 100- and 500-year event-based deposition modelling of flood events and long-term modelling using the 64 historical flood events between 1941 and 2014. The principal observations of this work are the followings:

- Hydrodynamic simulation results indicate that floodplain provides up to 23% attenuation to the largest recorded historical flood event (December 22, 1964 circa. 30-year return period) due to flood storage in the restored flood basin. The results also show that the 500-year flood event (115 m³/s) experiences a 28% flood peak reduction at the downstream (80 m³/s) which results in the equivalent of a 50-year flood magnitude. The East Lents floodplain's unique geomorphic features create substantial off-line flood storage. The floodplain behaves

in some way more like an alluvial fan than floodplain in the typical sense, therefore, it is still for 500-year flood event. Thus, the common assumption of floodplain restoration being only effective up to medium flow events (50-year) does not always hold as it depends on a number of factors including landscape features of the flood basin and hydrograph characteristics.

- This study proposes long-term hydro-morphodynamic simulation to evaluate the long-term impact of sediment deposition in the flood basin. This is the first quantitative methodology to account for long-term sediment aggradation in the restored floodplain using two-dimensional hydro-morphodynamic model. Hydro-morphodynamic simulation results indicate that ~20%–30% of sediment generated from the upstream is deposited in the East Lents floodplain, this sediment trapping considerably reduces the cumulative sediment loading into the Willamette River. On the other hand, as pollutants from road networks and agricultural land are attached to fine sediments, the East Lents flood plain soils may potentially show increased levels of contaminants over a long period

of time. However, there is no evidence whatsoever that sediments trapped in the East Lents floodplain pose any hazard due to contamination at present.

- During long-term simulation, part of the sediment deposited from the previous events are re-suspended; however, they largely remain deposited in the floodplain and shifted towards the lower region of the flood basin in the downstream direction. The results shows that during moderate (5–25 year) flow events sediments tend to concentrate at lower elevations of the flood basin, while larger events re-suspended the previously deposited sediments, spreading them across the flood basin.
- At the end of the 64 event long-term simulation, 2000 m^3 of sediment was deposited in the flood basin, which is equivalent to 0.4 metric ton/km^2 at the Sycamore gauging station. In other words, the sediment trapping at the East Lents flood basin reduces the annual sediment loading from Johnson Creek into the Willamette River by 1%, this provides both improved water quality and flood resilience benefits. Furthermore, deposited sediment over the simulated period (1941–2014) is approximately 0.1% of the basin's storage capacity. Hydrodynamic simulation results show that this storage reduction has very little impact on the flood basin's current flood attenuation capacity.

Floodplain restoration projects should not only be driven by socio-economic drivers, they should also be undertaken within a process-driven and integrated strategic framework by taking into account the downstream effects and long-term impacts on the system. These types of long-term numerical modelling studies will greatly increase the body of knowledge in floodplain restoration and may help managers better assess the time scale needed to determine whether a floodplain has been successfully restored.

Acknowledgements

References

Allen D., Arthur S., Haynes H., Mant J., Terrell R., Aspray T., Morse J. & Yeakley A. Urban catchment composition influence on storm water quality: green space, road and land use impact on urban waterway pollution. *Environmental Management*, submitted.

Archer D. Flood wave attenuation due to channel and floodplain storage and effects on flood frequency. In: K. Beven & P. A. Carling, eds. *Floods: hydrological, sedimentological and geomorphological implications*. Chichester: John Wiley & Sons, 1989, 37–46.

Ashmore P.E. & Day T.J. Spatial and temporal patterns of suspended-sediment yield in the Saskatchewan River basin. *Can J Earth Sci* 1988, **25**, 1450–1463.

Beasley G. & Kneale P. Reviewing the impact of metals and PAHs on macro invertebrates in urban watercourses. *Prog Phys Geogr* 2002, **26**, (2), 236–270.

Bilotta G.S. & Brazier R.E. Understanding the influence of suspended solids on water quality and aquatic biota. *Water Res* 2008, **42**, 2849–2861.

Booth D. Challenges and prospects for restoring urban streams: a perspective from the Pacific Northwest of North America. *J North Am Benthol Soc* 2005, **24**, (3), 724–737.

Chang H. Streamflow characteristics in urbanizing basins in the Portland Metropolitan Area, Oregon, USA. *Hydrol Process* 2007, **21**, (2), 211–222.

Chang H. & Franczky J. Climate change, land use change, and floods: toward an integrated assessment. *Geog Compass* 2008, **2**, (5), 1549–1579.

Chang H., Lafrenz M., Jung I.W., Figliozzi M., Platman D. & Pederson C. Potential impacts of climate change on flood-induced travel disruption: a case study of Portland in Oregon, USA. *Ann Assoc Am Geogr* 2010, **100**, (4), 938–952.

Chen H.J. & Chang H. Response of discharge, TSS, and E. coli to rainfall events in urban, suburban, and rural watersheds. *Environ Sci Process Impacts* 2014, **16**, (10), 2313.

Christine P., Jerzy S., Hanna W. & Krzysztof R. Dynamic Slow Down: a flood mitigation strategy complying with the integrated management concept – implementation in a small mountainous catchment. *Intl J River Basin Manage* 2005, **3**, (2), 75–85.

Dalton M.M., Mote P. & Snover A.K. Climate change in the Northwest: implications for our landscapes. In: *Waters, and communities*. Washington, DC: Island Press, 2013, 224 pp.

Dodds W.K. & Whiles M.R. Quality and quantity of suspended particles in rivers: Continent-Scale Patterns in the United States. *Environ Manage* 2004, **33**, (3), 355–367.

Evans E.P., Simm J.D., Thorne C.R., Arnell N.W., Ashley R.M., Hess T.M., Lane S.N., Morris J., Nicholls R.J., Penning-Rowsell E.C., Reynard N.S., Saul A.J., Tapsell S.M., Watkinson A.R. & Wheater H.S. *An update of the Foresight Future Flooding 2004 qualitative risk analysis*. London: Cabinet Office, 2008.

Federal Emergency Management Agency (FEMA). *Flood insurance study*. City of Portland, Oregon, Multnomah, Clackamas, and Washington Counties, revised October 19, 2004.

Finkenbine J.K., Atwater J.W. & Mavinic D.S. Stream health after urbanisation. *J Am Water Resour Assoc* 2000, **36**, (5), 1149–1159.

Fletcher T.D., Vietz G. & Walsh C.J. Protection of stream ecosystems from urban storm water runoff: the multiple benefits of an ecohydrological approach. *Prog Phys Geogr* 2014, **38**, (5), 543–555.

Fokkens B. The Dutch strategy for safety and river flood prevention. In: O.F. Vasiliev, P.H.A.J.M. van Gelder, E.J. Plate, & M.V. Bolgov, eds. *Extreme hydrological events: new concepts for security*, Vol. **78**. Springer Netherlands: Nato Science Series: IV, 2007, 337–352.

Guan M., Wright N.G. & Sleigh P.A. 2D process-based morphodynamic model for flooding by noncohesive dyke breach. *J Hydraul Eng* 2014, **140**, (7), 04014022.

Guan M., Wright N.G. & Sleigh P.A. Multimode morphodynamic model for sediment-laden flows and geomorphic impacts. *J Hydraul Eng* 2015a, **141**, (6), 04015006.

Guan M., Wright N.G., Sleigh P.A. & Carrivick J.L. Assessment of hydro-morphodynamic modelling and geomorphological impacts of a sediment-charged jökulhlaup, at Sólheimajökull, Iceland. *J Hydrol* 2015b, **530**, 336–349.

Habersack H., Jager E. & Hauer C. The status of the Danube River sediment regime and morphology as a basis for future basin management. *Int J River Basin Manage* 2013, **11**, (2), 153–166.

Hardy R.J., Bates P.D. & Anderson M.G. Modelling suspended-sediment deposition on a fluvial floodplain using a two-dimensional dynamic finite element model. *J Hydrol* 2000, **229**, 202–218.

Holmes N.T.H. & Nielsen M.B. Restoration of the rivers Brede, Cole and Skerne: a joint Danish and British EU-LIFE demonstration project, I – setting up and delivery of the project. *Aquatic Conserv: Mar Freshw Ecosyst* 1998, **8**, 185–196.

Hook A.M. & Yeakley J.A. Storm flow dynamics of dissolved organic carbon and total dissolved nitrogen in a small urban watershed. *Biogeochemistry* 2005, **75**, 409–431.

Hupp C.R., Pierce A.R. & Noe G.B. Floodplain geomorphic processes and environmental impacts of human alteration along coastal plain rivers, USA. *Wetlands* 2009, **29**, (2), 413–429.

Inman D.L. & Jenkins S.A. Climate change and the episodicity of sediment flux of small California Rivers. *J Geol* 1999, **107**, 251–70.

James C.S. Sediment transfer to overbank sections. *J Hydraul Res* 1985, **23**, 435–452.

Jung I.W., Chang H. & Moradkhani H. Quantifying uncertainty in urban flooding analysis considering hydroclimatic projection and urban development effects. *Hydrol Earth Syst Sci* 2011, **15**, (2), 617–633.

Kendrick M. The Thames barrier. *Landsc Urban Plan* 1988, **16**, (1–2), 57–68.

Klein R.D. Urbanisation and stream quality impairment. *Water Resour Bull* 1979, **15**, (4), 948–963.

Lane S.N. & Thorne C.R. River processes. In: C.R. Thorne, E.P. Evans, & E.C. Penning Rowell, eds. *Future flooding and coastal erosion risks*. London: Thomas Telford Publishing, 2007, 239–257, (ISBN: 978-0072773-449-5).

Lane S.N., Tayefi V., Reid S.C., Yu D. & Hardy R.J. *Earth Surf Process Landforms* 2007, **32**, 429–446.

Lee, K.K. and Synder, D.T. Hydrology of the Johnson Creek basin, Oregon. U.S. Geological Survey Scientific Investigation Report 2009-5123, 2009, 56 p.

Levell A. & Chang H. Monitoring the channel process of a stream restoration project in an urbanizing watershed: a case study of Kelley Creek, Oregon, USA. *River Res Appl* 2008, **24**, (2), 169–182.

May C.W., Horner R.R., Karr J.R., Mar B.W. & Welch E.B. Effects of urbanization on small streams in the Puget Sound ecoregion. *Watershed Prot Tech* 1997, **2**, (4), 483–494.

McIntyre, N & Thorne, C.R. Land use management effects on flood flows and sediments – guidance on prediction. FRMRC Research Report CIRIA C719, 2013, 113 p.

Moody J.A. & Troutman B.M. Quantitative model of the growth of floodplains by vertical accretion. *Earth Surf Process Landforms* 2000, **25**, 115–133.

Nanson G.C. & Croke J.C. A genetic classification of floodplains. In: G.R. Brakenridge & J. Hagedorn, eds. *Floodplain evolution*. Geomorphology, Elsevier Science Publishers B.V., Amsterdam Vol. **4**, 1992, 459–486.

National Weather Service (NWS). *Flood fatalities*. Hydrologic Information Center, 2016. Available at: www.nws.noaa.gov/hic (accessed on 5th February 2016)

Newcombe C.P. & Jensen J.O.T. Channel suspended-sediment and fisheries: a synthesis for quantitative assessment of risk and impact. *North Am J Fisheries Manage* 1996, **16**, (4), 693–727.

Nicholas A.P. & Walling D.E. Numerical modelling of floodplain hydraulics and suspended-sediment transport and deposition. *Hydrol Process* 1998, **12**, 1339–1355.

Niemczynowicz J. Urban hydrology and water management – present and future challenges. *Urban Water* 1999, **1**, (1), 1–14.

Nones M., Guerrero M. & Ronco P. Opportunities from low-resolution modelling of river morphology in remote parts of the world. *Earth Surf Dynam* 2014, **2**, 9–19.

O'Sullivan J.J., Ahilan S. & Bruen M. A modified Muskingum routing approach for floodplain flows: theory and practice. *J Hydrol* 2012, **470–471**, 239–254.

Pender D., Patidar S., Hassan K. & Haynes H. Method for incorporating morphological sensitivity into flood inundation modeling. *J Hydraul Eng* 2016, **146**, (6), 1–11, doi: 10.1061/(ASCE)HY.1943-7900.0001127.

Pizzuto J.E. Sediment diffusion during overbank flows. *Sedimentology* 1987, **34**, 301–317.

Porterfield G. Computation of fluvial-sediment discharge. In: *U. S. geological survey techniques of water resources investigations*, 1972. U.S. Geological Survey, 1200 South Eads Street, Arlington, VA 22202 Book 3, chap. C3, 66 p.

Pratt B. & Chang H. Effects of land cover, topography, and built structure on seasonal water quality at multiple spatial scales. *J Haz Mat* 2012, **209/210**, 48–58.

Rasmussen P.P., Gray J.R., Glysson G.D. & Ziegler A.C. Guidelines and procedures for computing time series suspended-sediment concentrations and loads from in-stream turbidity-sensor and streamflow data. In: *U.S. geological survey techniques and methods*, 2009, U.S. Geological Survey, Reston, Virginia book 3, chap. C4, 52 p.

van Rijin L.C. Sediment transport part II, suspended load transport. *J Hydraul Eng* 1984, **110**, 1613–1641.

Rohde S., Hostmann M., Peter A. & Ewald K.C. Room for rivers: an integrative search strategy for floodplain restoration. *Landsc Urban Plan* 2006, **78**, 50–70.

Roman D.C., Vogel R.M. & Schwarz G.E. Regional regression models of watershed suspended-sediment discharge for the eastern United States. *J Hydrol* 2012, **472–473**, 53–62.

Ronco P., Gallina V., Torresan S., Zabeo A., Semenzin E., Critto A. & Marcomini A. The KULTURisk regional risk assessment methodology for water-related natural hazards – Part 1: physical–environmental assessment. *Hydrol Earth Syst Sci* 2014, **18**, 5399–5414. doi: 10.5194/hess-18-5399-2014.

Salathé E.P. Jr., Hamlet A.F., Mass C.F., Lee S.Y., Stumbaugh M. & Steed R. Estimates of twenty-first-century flood risk in the Pacific Northwest based on regional climate model simulations. *J Hydrometeor* 2014, **15**, 1881–1899.

Savage, G. Sedimentation study report, Johnson Creek, Environmental services system analysis, 2005.

Singh S. & Chang H. Effects of land cover change on water quality in urbanizing streams at two spatial scales. *Int J Geospatial Environ Res* 2014, **1**, (1), Article 8, 1–21.

Sonoda K. & Yeakley J.A. Relative effects of land use and near-stream chemistry on phosphorus in an urban stream. *J Environ Qual* 2007, **36**, 144–154.

Sonoda K., Yeakley J.A. & Walker C.E. Near-stream land use effects on stream water nutrient distribution in an urbanizing watershed. *J Am Water Resour Assoc* 2001, **37**, 1512–1537.

Soulsby R. *Dynamics of marine sands: a manual for practical applications*. London: Thomas Telford, 1997, p. 249.

Stone M. & Droppo I.G. In-channel surficial fine-grained sediment laminae. Part II: chemical characteristics and implications for contaminant transport in fluvial systems. *Hydrol Process* 1994, **8**, 113–124.

Stonewall, A.J. & Bragg, H.M. Suspended-sediment characteristics for the Johnson Creek basin, Oregon, water years 2007–2010. U.S. Geological Survey Scientific Investigation Report 2012-5200, (2012) 32 p.

Thomas, N.A. (1987) Use of biomonitoring to control toxics in the United States. Environmental Protection Agency Technical, Report PB-88-107933/XAB; EPA-600/D-87/278, 11 p.

Timmins, K. and Wolff, G. East Lents Floodplain Restoration Project – Phase 2. Draft technical report, Otak Project No. 14781, 2012, 54 p.

U.S. Army Corps of Engineers (USACE). Johnson Creek Flooded Area Update, Portland District. *CENWP-EC-HY*, December, 1999.

U.S. Census Bureau. 2010. Available at: https://www.census.gov/newsroom/releases/archives/2010_census/cb12-50.html (accessed on 7th March 2015).

USEPA (US Environmental Protection Agency). National Water Quality Inventory 1998 Report to Congress. US Environmental Protection Agency, EPA 841-R-00-001, Office of Water, Washington, DC, 2000.

Willems P. Revision of urban drainage design rules after assessment of climate change impacts on precipitation extremes at Uccle, Belgium. *J Hydrol* 2013, **496**, 166–177.

Williamson S.C., Bartholow J.M. & Stalnaker C.B. Conceptual model for quantifying pre-smolt production from flow dependent physical habitat and water temperature. *Regula River Res Manage* 1993, **8**, 15–28.

Wolff C.G. & Burges S.J. An analysis of the influence of river channel properties on flood frequency. *J Hydrol* 1994, **153**, 317–337.

Woltemade C.J. & Potter K.W. A watershed modelling analysis of fluvial geomorphologic influences on flood peak attenuation. *Water Resour Res* 1994, **30**, (6), 1933–1942.

Wood P.J. & Armitage P.D. Biological Effects of Fine Sediment in the Lotic Environment. *Environ Manage* 1997, **21**, (2), 203–217.

Yeakley J.A. & Hughes R.M. Global and regional context of salmonids and urban areas. In: J.A. Yeakley, K.G. Maas-Hebner, & R.M. Hughes, eds. *Wild Salmonids in the urbanizing Pacific Northwest*. New York: Springer, 2014, 11–29.

Yeakley J.A., Maas-Hebner R.M. & Hughes R.M. *Wild Salmonids in the urbanizing Pacific Northwest*. New York: Springer, 2014, 271 pp.

Yorke, T.H. Herb W.J. Effect of Urbanisation on Streamflow and Sediment Transport in the Rock Creek and Anacostia River Basins, Montgomery County, Maryland, 1962–64, Geological Survey Professional paper, 1978.